Published in final edited form as:

Dev Dyn. 2015 November ; 244(11): 1404–1414. doi:10.1002/dvdy.24321.

Histone acetylation regulates prostate ductal morphogenesis through a BMP dependent mechanism

Kimberly P. Keil[1], **Helene M. Altmann**[1], **Lisa L. Abler**[1], **Laura L. Hernandez**[2], and **Chad M. Vezina**[1]

[1]Department of Comparative Biosciences, University of Wisconsin-Madison, Madison Wisconsin 53706

[2]Department of Dairy Science, University of Wisconsin-Madison, Madison, WI 53706

Abstract

Background—Epigenetic factors influence stem cell function and other developmental events but their role in prostate morphogenesis is not completely known. We tested the hypothesis that histone deacetylase (HDAC) activity is required for prostate morphogenesis.

Results—We identified the presence of class I nuclear HDACs in the mouse urogenital sinus (UGS) during prostate development and found that *Hdac 2* mRNA abundance diminishes as development proceeds which is especially evident in prostatic epithelium. Blockade of HDACs with the inhibitor trichostatin A (TSA) decreased the number of prostatic buds formed in UGS explant cultures but not the number of buds undergoing branching morphogenesis. In the latter, TSA promoted an extensive branching phenotype that was reversed by exogenous NOGGIN protein, which functions as a bone morphogenetic protein (BMP) inhibitor. TSA also increased *Bmp2* promoter H3K27ac abundance, *Bmp2* and *Bmp4* mRNA abundance, and the percentage of epithelial cells marked by BMP-responsive phosphorylated SMAD1/5/8 protein. TSA exposed UGS explants grafted under the kidney capsule of untreated host mice for continued development achieved a smaller size without an obvious difference in glandular histology compared to control treated grafts.

Conclusions—These results are consistent with an active role for HDACs in shaping prostate morphogenesis by regulating *Bmp* abundance.

Graphical Abstract

Corresponding author: Chad Vezina, 1656 Linden Dr., Madison WI, 53705, cmvezina@wisc.edu.

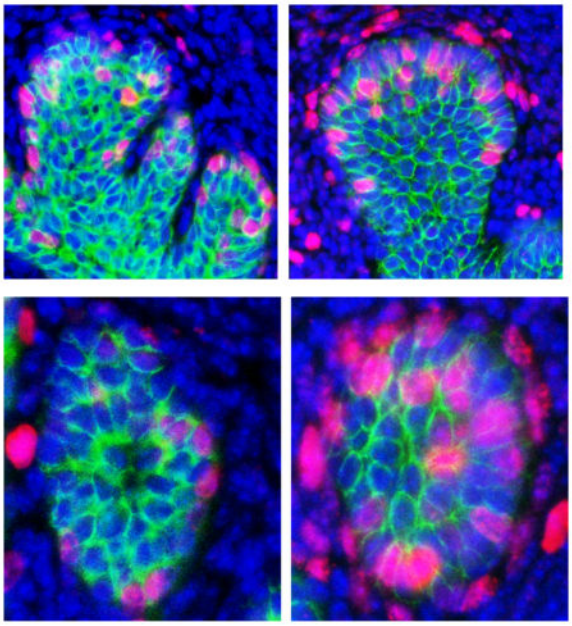

Keywords

Trichostatin A; chromatin; urogenital sinus

Introduction

The prostate develops from a compartment of the lower urinary tract known as the urogenital sinus (UGS). Androgen receptor (AR) activation in UGS mesenchyme instructs UGS epithelium to form prostatic buds which elongate into surrounding mesenchyme (Cunha, 1985). Mouse prostatic bud initiation occurs at 16–18 days post coitus (dpc) in a characteristic pattern that determines the position of anterior, dorsal, lateral and ventral prostate lobes (Lin et al., 2003). Prostatic buds elongate and undergo branching morphogenesis which is completed around postnatal day (P) 20 and is characterized by unique branching patterns in each prostatic lobe (Sugimura et al., 1986; Prins et al., 2006).

Epigenetic modifications are likely to serve an important regulatory mechanism in prostate development. For example, we recently showed that DNA methylation determines *Ar* and E-cadherin abundance during the onset and progression of prostatic bud formation (Keil et al., 2014a; Keil et al., 2014b). Other epigenetic modifications, such as histone acetylation/deacetylation, are also powerful regulators of gene expression but their roles in prostate development have not been examined. Histone acetyl transferases (HATs) add acetyl groups to lysine residues of histone tails, typically resulting in transcriptional activation while histone deacetylases (HDACs) remove acetyl groups typically resulting in gene silencing. Histone deacetylation regulates the expression of some important morphogens. For example, during unilateral ureteral obstruction, histone deacetylation represses bone morphogenic protein 7 (*Bmp7*) expression, which is reversed by the HDAC inhibitor trichostatin A (TSA) (Manson et al., 2014).

Budding and branching morphogenesis in the prostate and other organs requires fine tuning and localized action of BMPs. BMP4 and BMP7 inhibit prostatic bud formation and branching morphogenesis by decreasing proliferation and limiting the effects of growth promoting signals like fibroblast growth factor 10 (Lamm et al., 2001; Grishina et al., 2005; Cook et al., 2007; Buresh-Stiemke et al., 2012). BMP inhibitory actions on prostate development are in part responsible for establishing periodicity of prostatic buds and patterns of branched ductal tips (Mehta et al., 2011). BMP signaling also regulates prostate luminal epithelial differentiation (Omori et al., 2014). Some transcriptional regulators of BMP signaling in developing prostate are known. For example, BMP transcription is stimulated by beta-catenin signaling and repressed by retinoic acid signaling (Mehta et al., 2013, Vezina et al., 2008). How these factors regulate BMP expression, and if chromatin modifications such as histone acetylation and deacetylation are involved, have not been determined.

In this study, we tested the hypothesis that histone deacetylation is required for prostate development. *Hdacs1-3* are expressed in developing prostate mesenchyme and epithelium in a pattern that overlaps that which has been described previously for *Bmp2*, *4*, and *7* mRNAs (Lamm et al., 2001; Grishina et al., 2005; Cook et al., 2007; Mehta et al., 2013). An HDAC inhibitor decreases the total number of prostatic buds that form from UGS explant cultures. Although the HDAC inhibitor does not change the percentage of prostatic buds undergoing branching morphogenesis, it causes an extensive branching phenotype in buds undergoing branching morphogenesis. Chemical inhibition of HDACs increases *Bmp2* and *Bmp4* transcript abundance and *Bmp2* promoter histone H3 lysine 27 acetylation (H3K27ac). Addition of BMP antagonist NOGGIN partially restores budding and branching morphogenesis in prostate explants treated with HDAC inhibitor. Together these results suggest that HDACs are indeed critical regulators of prostate development and exert their actions at least in part by regulating *Bmp* chromatin structure and expression.

Results

Hdacs 1-3 are present in developing prostate mesenchyme and epithelium during prostatic bud formation and diminish during branching morphogenesis

We focused our study on nuclear class 1 *Hdacs* which are known to regulate cell proliferation and survival (Dokmanovic et al., 2007). We investigated relative abundance of *Hdacs 1-3* across the whole male UGS at 17 days post coitus (dpc) and postnatal day (P) 5 by QPCR. *Hdac2* abundance was significantly reduced during the period from 17 dpc to P5, while *Hdac 1* and *3* abundance did not significantly change during this period (Fig. 1C,F,I). *In situ* hybridization (ISH) was performed to determine the spatial and temporal expression of *Hdacs 1-3* on 17 dpc and P5 male lower urinary tract sections. Immunohistochemistry (IHC) was also performed on sections to visualize epithelium using an anti-E-cadherin (CDH1) antibody. *Hdacs 1-3* are expressed in prostate mesenchyme and epithelium and exhibit changes in spatial localization during prostatic bud elongation and branching morphogenesis. *Hdac 1* is predominantly expressed in mesenchyme adjacent to prostatic buds and urethral epithelium, the so called peri-prostatic and lamina propria mesenchyme (Fig. 1A). This pattern persists to at least postnatal day (P) 5 (Fig. 1B). *Hdac 2* and *Hdac 3*

are predominantly expressed in prostatic epithelium at 17 dpc but are no longer detected in prostatic epithelium by P5 (Fig. 1D–E, G–H).

HDAC inhibition decreases prostatic budding and alters branching morphogenesis

To determine the role of histone acetylation during budding and branching morphogenesis, we pharmacologically inhibited HDACS (class I and II) with trichostatin A (TSA). *In vitro* explant cultures have widely been used in prostate developmental studies. *In vitro* development recapitulates androgen dependent budding and branching morphogenesis observed *in vivo* and additionally allows androgen and other pharmacological inhibitors to be introduced in defined concentrations and at specific developmental stages (Doles et al., 2005). Using this approach, 14 dpc prostate explants were cultured in media containing androgen (10nM dihydrotestosterone, DHT) and vehicle control (0.1% DMSO) or vehicle containing increasing concentrations of TSA (1–100nM). Explants were then stained by ISH to visualize the prostatic marker NK-3 transcription factor locus 1 (*Nkx3-1*) and by IHC using an antibody against CDH1 to visualize epithelium (Fig. 2A) (Keil et al., 2012a). TSA treatment (10–100nM) significantly decreased prostatic bud number (Fig. 2B). The number of prostatic buds undergoing branching morphogenesis significantly increased in the 10nM TSA group but was not affected in the 50–100nM groups (Fig. 2C). Interestingly, TSA (100nM) caused an extensive branching phenotype in prostatic buds undergoing branching morphogenesis, which was marked by an increase in the number of distal tips per bud (Fig. 2D). These results indicate that histone acetylation is likely to regulate prostatic bud number and branching morphogenesis.

HDAC inhibition increases *Bmp2* and *4* mRNA abundance in developing prostate

To uncover the underlying mechanism for TSA action, we examined abundance of *Bmp2*, *4*, *7* mRNAs, which are expressed during prostatic bud formation (Lamm et al., 2001; Grishina et al., 2005; Cook et al., 2007) and abundance of *Bmp6*, which is overexpressed in prostate cancer (Dai et al., 2005). TSA treatment significantly increases *Bmp2* and *Bmp4* mRNA abundance in UGS explants (Fig. 3 A,B) without significantly changing abundance of *Bmp6* or *Bmp7* (Fig. 3 C,D). Since histone acetylation is typically associated with transcriptional activation, we tested whether TSA also increases the activating mark H3K27 acetylation at *Bmp2* and *Bmp4* genetic loci. Using chromatin immunoprecipitation (ChIP) we found that TSA significantly increases *Bmp2* but not *Bmp4* H3K27 acetylation in the genetic regions examined (Fig. 3 E,F). We next tested whether TSA increases *Bmp* signaling in UGS explants by quantifying abundance of the downstream target phosphoSMAD1/5/8 (pSMAD1/5/8). There were significantly more prostatic bud epithelial cells and more peri-prostatic mesenchyme cells marked by detectable pSMAD1/5/8 immunostaining in TSA treated UGS explants compared to control explants (Fig. 4 A–C). These results indicate that an HDAC inhibitor increases BMP signaling in prostatic bud tips and surrounding mesenchyme.

Exogenous BMP2 mimics effects of TSA on branching morphogenesis

Since TSA increased abundance of *Bmp2* mRNA and H3K27 acetylation marks, and since roles for *Bmp2* in prostate development have not been examined, we focused the next study

on a potential role of this molecule in prostate development. 14 dpc prostate explants were cultured for 7d in media containing androgen (10nM DHT) and graded concentrations of exogenous human BMP2 protein (1–1000nM). Fetal prostate explants were stained by ISH for *Nkx3-1* and IHC and prostatic buds counted as described above (Fig. 5A). Exogenous BMP2 did not significantly change the number of prostatic buds formed (Fig. 5B) or the number of buds undergoing branching morphogenesis (Fig. 5C) but did cause excessive branches to form in prostatic buds undergoing branching morphogenesis at the 100ng/ml concentration (Fig. 5D).

A BMP inhibitor rescues TSA induced changes in prostatic branching morphogenesis

We next tested whether a BMP inhibitor would antagonize TSA effects on prostate ductal morphogenesis. We used recombinant NOGGIN, a peptide inhibitor that binds and sequesters BMPs to prevent them from activating their receptors. 14 dpc male UGS explants were cultured for 7d in media containing androgen (10nM DHT) and either TSA (100nM), recombinant NOGGIN (5μg/ml) or both. This NOGGIN concentration was used previously in mouse prostate explant culture to antagonize BMP signaling (Cook et al., 2007; Mehta et al., 2013). TSA treatment alone increased prostatic bud tips per branching bud but this effect was blocked by exogenous NOGGIN (Fig. 6A–B). Therefore, we conclude that the excessive branching phenotype caused by TSA is mediated in part by enhanced BMP signaling.

HDAC inhibition does not significantly impact prostatic ductal maturation

We tested whether HDAC inhibition during prostatic bud formation and the early period of branching morphogenesis caused enduring effects on prostate glandular development, differentiation and ductal maturation. 14 dpc male mouse UGS explants were grown 7d in medium containing androgen (10nM DHT) and either vehicle or vehicle containing TSA (100nM). Explants were then transplanted under the renal capsule of an intact adult male syngeneic host mouse and grown for an additional month, a sufficient length of time for glandular development (Doles et al., 2005). Importantly, the host mouse was not treated with TSA. We discovered that TSA exposed grafts were smaller than control grafts after a month of growth under the renal capsule (Fig. 7A–B). However, despite having a smaller volume, TSA treated grafts formed histologically normal ducts (Fig. 7C). Grafts from both treatment groups expressed comparable amounts of smooth muscle actin, AR, epithelial markers cytokeratin 14 and 8, and prostate secretory product probasin (Fig. 7D–H). Thus despite their smaller volumes, TSA exposed tissue grafts undergo apparently normal differentiation and form a ductal network capable of producing adult prostate secretory products. These results indicate the developmental changes observed with TSA affect glandular complexity but not cell differentiation.

Discussion

Epigenetic modifications such as DNA methylation have been shown to regulate AR to control the timing and onset of prostatic bud formation (Keil et al., 2014a) and regulate e-cadherin to regulate prostatic bud outgrowth (Keil et al., 2014b). Roles for other epigenetic modifications such as histone acetylation have never been examined in developing prostate.

Here we show that expression of mRNAs encoding enzymes responsible for histone deacetylation are expressed in mesenchyme and epithelium of developing prostate during prostatic bud formation and diminish during branching morphogenesis. We reveal a role for HDACS in regulating prostatic budding and branching morphogenesis in part by regulating BMP expression. Inhibition of HDACS decreases total prostatic bud number, increases the extent of branching in prostatic buds undergoing branching morphogenesis, and increases *Bmp2* H3K27ac and mRNA expression. Increased BMP signaling is in part responsible for altered branching morphology since inhibition of BMP signaling partially rescues the branching abnormality seen in tissues treated with the HDAC inhibitor. Together these results indicate that HDACs act to temporally and spatially restrain the inhibitory actions of BMPs during prostatic budding and branching morphogenesis (Fig. 8).

Several pathways have been shown to shape BMP expression in the developing prostate. Overexpression of beta-catenin in developing mouse prostate epithelium induces BMP2, 4, and 7 expression and represses prostatic bud formation (Mehta et al., 2013). Retinoic acid signaling decreases *Bmp4* expression and enhances prostatic bud formation (Vezina et al., 2008). Mice deficient in *Noggin* develop fewer prostatic buds than wild type controls (Cook et al., 2007). Mice with conditional BMP receptor 1a deletion during prostate development are deficient in epithelial differentiation and ductal maturation and in adulthood exhibit hyperplasia and inflammation (Omori et al., 2014). Stromal TGF-β increases BMP6 in prostate stromal cells and is in part responsible for inducing AR activity (Yang et al., 2014). While some of these factors act directly to control BMP expression, mechanisms by which paracrine-acting factors determine BMP abundance are less well understood. Our results are the first to identify histone deacetylation as an epigenetic mechanism that determines BMP abundance in developing prostate. Expression patterns of *Hdac1-3* overlap temporally and spatially with *Bmp*s, especially at developing prostatic bud tips and peri-prostatic mesenchyme (Lamm et al., 2001; Grishina et al., 2005; Cook et al., 2007; Mehta et al., 2013). A histone deacetylase inhibitor increases *Bmp2* and *4* transcript abundance, inhibits prostatic budding and increases tips per branched bud. These results are in line with those found in kidney, where histone deacetylation negatively regulates *Bmp7* expression (Manson et al., 2014). Whether signaling pathways known to alter BMP expression induce changes in *Bmp* histone acetylation or whether inhibition of histone deacetylation alters beta-catenin signaling, retinoic acid signaling or *Noggin* expression to induce *Bmps* is unknown and a future area of study.

Fine tuning of BMP signaling dictates both number and patterning of budding and branching morphogenesis in prostate and other organs (Zhang et al., 2008; Chi et al., 2011; Mehta et al., 2013). In the prostate *Bmp2, Bmp4* and *Bmp7* are expressed in epithelium and mesenchyme especially in peri-prostatic mesenchyme (Lamm et al., 2001; Grishina et al., 2005; Mehta et al., 2013). *Bmp4* and *Bmp7* are inhibitors of prostatic bud formation and branching morphogenesis (Lamm et al., 2001; Grishina et al., 2005; Cook et al., 2007; Mehta et al., 2013). Our results are the first to examine the role of exogenous BMP2 on *in vitro* prostatic bud formation. Unlike BMP4 and BMP7 which are inhibitory to prostatic budding and branching, BMP2, at the concentrations tested in this study, selectively influences prostatic branching morphogenesis. Exogenous BMP2 did not alter the total

number of prostatic buds formed, or number of buds undergoing branching morphogenesis, but instead caused excessive branches to form in prostatic buds undergoing branching morphogenesis. Our study is not the first to suggest differential roles for BMP2 and BMP4 in morphogenesis; this has also been observed in the kidney. While BMP4 is inhibitory to kidney growth and branching morphogenesis, BMP2 does not alter number of glomeruli formed and though not significant, BMP2 trends toward increasing the number of branch tips from metonephri grown in the presence of exogenous BMP2 (1–10nM) (Martinez et al., 2002). Whether a concentration of BMP2 similar to that used in our study (100nM) would produce a significant increase is possible. Together these results provide evidence of a role for BMP2 primarily in the patterning of branching morphogenesis. Our results now indicate that the epigenome, and specifically histone deacetylation plays a role in fine tuning BMP signaling to direct the course of prostate morphogenesis.

In this study we use TSA as a tool to examine changes in histone acetylation and prostate development. Like all pharmacological agents, TSA can have off-target or downstream effects. TSA is an inhibitor of class I and class II HDAC's. Thus the effects of TSA on prostatic budding observed in this study could be occurring through changes in HDACs other than those examined here (*Hdac 1-3*). How HDACS are regulated and which HDACS regulate BMP expression and prostate morphogenesis remains to be determined. Similarly, some HDACS function outside of the nucleus and thus have other targets besides transcriptional regulation via chromatin (Dokmanovic et al., 2007). For example, TSA can also inhibit transcription factor deacetylation thus altering protein interactions and complex formation (Glozak et al., 2005). Despite these factors we demonstrate that in vitro administration of TSA to induce changes in branching morphology are reversed by co-administration with NOGGIN, demonstrating a link to BMP signaling.

This study focused on histone deacetylation roles in prostatic bud formation and branching morphogenesis. How changes in prostate morphology during development affect prostate morphogenesis in adulthood or disease is not completely understood. Our results indicate that TSA administration during prostate development decreases prostatic bud number and alters branching complexity. When these same tissues are grown as xenografts, they have diminished volume compared to control grafts. Based on these results it is possible that changes to prostatic bud number during development may contribute to overall prostatic volume in adulthood. Interestingly, despite the effects of TSA on diminished graft volume these tissues go on to differentiate and form mature ducts. One possibility to explain this is the continued expression of BMPs. This is supported by the fact that conditional BMP receptor 1a deletion in developing prostate leads to impaired prostate differentiation and maturation (Omori et al., 2014).

It is likely that HDACs continue to regulate BMP abundance and prostate homeostasis in adulthood and during prostate cancer. HDAC expression is higher in prostate cancer compared to benign tissue and HDAC1 and 2 expression positively correlates with Gleason score (Patra et al., 2001; Weichert et al., 2008). Consequently, histone deacetylase inhibitors, including TSA alone or in combination with other therapies, have been a focus of anti-cancer therapeutics in prostate and other cancers (Marks, 2010). HDAC inhibitors have been shown to decreases epithelial to mesenchymal transition in prostate cancer cell lines

(Wang et al., 2015) and sensitize prostate stem-like cells to radiation (Frame et al., 2013). Clinical trials with HDAC inhibitors have shown some promise with reduction in PSA levels (Molife et al., 2010; Rathkopf et al., 2010) but overall little benefit in patients with prostate cancer is seen in part due to toxicity and drug delivery issues (Rathkopf et al., 2010; Pili et al., 2012; Schneider et al., 2012; Rathkopf et al., 2013). Targeting HDAC inhibitors to cancer cells by conjugating secondary agents able to bind androgen receptor are now being evaluated to improve delivery of HDACs to cancer cells while decreasing off-target cytotoxic effects (Gryder et al., 2013).

Our study focuses on BMP signaling as a target of histone deacetylation during prostatic bud formation and early branching morphogenesis. In other developing organs, histone acetylation has been implicated in regulation of fibroblast growth factors, sonic hedgehog, transforming growth factor beta, and notch(Xu et al., 2000), all of which are critical prostate morphogens. Testing whether histone acetylation controls these factors in developing prostate is an area of future study. Overall, we reveal that histone deacetylation may act as a reversible means to temporally and spatially regulate BMP signaling to control prostate bud number as well as shape branching morphogenesis.

Experimental Procedures

Animals

Wild type C57BL/6J mice were purchased from Jackson Laboratory (Bar Harbor, ME) and housed as described previously (Keil et al., 2012a). All procedures were approved by the University of Wisconsin Animal Care and Use Committee and conducted in accordance with the NIH Guide for the Care and Use of Laboratory Animals. To obtain timed-pregnant dams, females were paired overnight with males. The next morning was considered 0 days post coitus (dpc). Pregnant dams were euthanized by CO_2 asphyxiation and UGS tissue collected from resulting fetuses.

In situ hybridization (ISH)

ISH was conducted on whole mount tissues as described previously (Abler et al., 2011; Keil et al., 2012a). Detailed protocols for PCR-based riboprobe synthesis are available at www.gudmap.org. Staining patterns were assessed in at least three litter independent tissues per group. Tissues were processed as a single experimental unit to allow for qualitative comparisons among biological replicates and treatment groups.

Organ Culture

Male 14 dpc mouse urogenital sinus (UGS) explants were placed on 0.4-μm Millicell-CM filters (Millipore, Billerica, MA) and cultured as described previously. Medium was supplemented with one or all of the following: 10 nM 5α-dihydrotestosterone (DHT), 0.1% dimethyl sulfoxide (DMSO, vehicle control), DMSO containing 1–1000ng/ml trichostatin A (TSA, T8552, Sigma-Aldrich, St. Louis, MO), exogenous human BMP2 (1–1000ng/ml, 355-BM-010, R&D Systems, Minneapolis, MN), or recombinant NOGGIN (5μg/ml, 6057-NG-025, R&D Systems). Medium and supplements were changed every 2 days.

Immunohistochemistry (IHC)

Immunofluorescent staining of ISH-stained tissues and paraffin sections was performed as described previously. Primary antibodies were diluted as follows: 1:200 rabbit anti-CDH1 (3195, Cell Signaling Technology, Beverly, MA), 1:250 mouse anti-CDH1 (610181, BD Transduction Laboratories, San Jose, CA), 1:100 rabbit anti-phosphoSMAD1/5/8 (9511, Cell Signaling Technology, Danvers, MA). Secondary antibodies were diluted as follows: 1:250 Dylight 549-conjugated goat anti-rabbit IgG (111-507-003, Jackson ImmunoResearch, West Grove, PA), and 1:250 Dylight 488-conjugated goat anti-mouse IgG (115-487-003, Jackson ImmunoResearch). Immunofluorescently labeled tissues were counterstained with 4',6-diamidino-2-phenylindole, dilactate (DAPI), and mounted in anti-fade medium (phosphate buffered saline containing 80% glycerol and 0.2% n-propyl gallate). Whole mount immunohistochemistry was performed as described previously. Primary antibody was diluted 1:750 rabbit anti-CDH1 and secondary antibody was diluted 1:500 biotin conjugated goat anti-rabbit IgG (BA-1000, Vector, Burlingame, CA).

Chromatin Immunoprecipitation (ChIP)

UGS explants were pooled (5–6 tissues/pool) and each experimental group consisted of at least three pools. ChIP was conducted with modifications to the methylated DNA immunoprecipitation (MeDIP) protocol described previously for developing prostate (Keil et al., 2014b). All buffers contained protease inhibitor cocktail (Sigma P8340, 1ulPIC:200ul Buffer). Tissues were homogenized in lysis buffer (0.1M NaCl, 5mM EDTA, 50mM Tris-HCl pH8) using a pestle followed by continuous vortexing with stainless steel beads for 5 minutes. Homogenates were passed through an 18G needle and sonicated using a tip sonicator (setting 11, 15 sec on 45 sec off for 15 rounds). Agarose gel electrophoresis on 10ul of sample was used to verify chromatin fragmentation to a length corresponding to 200–1000bp of a double stranded DNA ladder. 300ug chromatin diluted in ChIP buffer (0.01%SDS, 1.1% Triton X-100, 1.2mM EDTA, 16.7mM Tris-HCl pH 8.1, 167mM NaCl) to 0.5 ml was used per IP. Samples were split into two tubes, with 10% of the divided fraction saved as input control. One fraction was incubated with 1ug anti-mouse H3K27ac (ab4729, Abcam, Cambridge, MA), the other with anti-mouse IgG control (ab18413, Abcam) antibody; both fractions were incubated overnight at 4ºC. Conjugated antibody was captured using protein A agarose salmon sperm DNA beads 30μl/ml (#16-157, Millipore, Billerica, MA) for 2 hours at 4ºC. Beads were washed with low salt buffer (0.1% SDS, 1% Triton X-100, 2mM EDTA, 20mM Tris-HCl pH 8.1, 150mM NaCl), high salt buffer (0.1% SDS, 1% Triton X-100, 2mM EDTA, 20mM Tris-HCl pH 8.1, 500mM NaCl) and lithium chloride buffer (0.25M LiCl, 1% IGEPAL-CA630, 1% deoxycholic acid (sodium salt), 1mM EDTA, 10mM Tris pH 8.1). Precipitated chromatin and 10% input was incubated in elution buffer (1% SDS, 0.1M NaHCO3, 200mM NaCl, 0.05mg/ml Proteinase K) at 65ºC for 4 hours, supernatant was collected and DNA purified using Qiagen PCR Purification kit according to manufacturer's instructions. Real time quantitative PCR (QPCR) was performed as described previously using gene specific primers listed in Table 1. Results were analyzed using the ΔΔCt method as described previously and expressed as enrichment over IgG (Livak and Schmittgen, 2001).

Real Time Quantitative PCR (QPCR)

QPCR was conducted as described previously (Keil et al., 2012b) on UGS explant pools (5–6 tissues/pool) with five pools per experimental treatment group using the gene specific primers listed in Table 1. Relative mRNA abundance was determined by the ΔΔCt method as described previously and normalized to peptidyl prolyl isomerase a (*Ppia)* abundance (Livak and Schmittgen, 2001).

Statistical analyses

For prostatic bud counting, UGSs were stained by ISH for *Nkx3-1* mRNA and counted as described previously. For immunolabeled cell counting, pSMAD1/5/8 positive cells were counted in at least two sections from three litter independent tissues per treatment group. Statistical analysis was performed using R version 2.13.1. Homogeneity of variance was determined using Levene's test. Student's T-test, one way analysis of variance (ANOVA), followed by Tukey's Honest Significant Difference (HSD) were used to identify significant differences ($p \leq 0.05$) between or among treatment groups.

Supplementary Material

Refer to Web version on PubMed Central for supplementary material.

Acknowledgments

Grant information: This work was supported by National Institutes of Health Grant R01DK099328 (cmv). The content is solely the responsibility of the authors and does not necessarily represent the official views of the National Institutes of Health.

References

Abend A, Kehat I. Histone deacetylases as therapeutic targets - From cancer to cardiac disease. Pharmacol Ther. 2014

Abler LL, Mehta V, Keil KP, Joshi PS, Flucus CL, Hardin HA, Schmitz CT, Vezina CM. A high throughput in situ hybridization method to characterize mRNA expression patterns in the fetal mouse lower urogenital tract. J Vis Exp. 2011

Buresh-Stiemke RA, Malinowski RL, Keil KP, Vezina CM, Oosterhof A, Van Kuppevelt TH, Marker PC. Distinct expression patterns of Sulf1 and Hs6st1 spatially regulate heparan sulfate sulfation during prostate development. Dev Dyn. 2012; 241:2005–2013. [PubMed: 23074159]

Chi L, Saarela U, Railo A, Prunskaite-Hyyrylainen R, Skovorodkin I, Anthony S, Katsu K, Liu Y, Shan J, Salgueiro AM, Belo JA, Davies J, Yokouchi Y, Vainio SJ. A secreted BMP antagonist, Cer1, fine tunes the spatial organization of the ureteric bud tree during mouse kidney development. PLoS One. 2011; 6:e27676. [PubMed: 22114682]

Cook C, Vezina CM, Allgeier SH, Shaw A, Yu M, Peterson RE, Bushman W. Noggin is required for normal lobe patterning and ductal budding in the mouse prostate. Dev Biol. 2007; 312:217–230. [PubMed: 18028901]

Cunha GR. Mesenchymal-epithelial interactions during androgen-induced development of the prostate. Prog Clin Biol Res. 1985; 171:15–24. [PubMed: 3885244]

Dai J, Keller J, Zhang J, Lu Y, Yao Z, Keller ET. Bone morphogenetic protein-6 promotes osteoblastic prostate cancer bone metastases through a dual mechanism. Cancer Res. 2005; 65:8274–8285. [PubMed: 16166304]

Dokmanovic M, Clarke C, Marks PA. Histone deacetylase inhibitors: overview and perspectives. Mol Cancer Res. 2007; 5:981–989. [PubMed: 17951399]

Doles JD, Vezina CM, Lipinski RJ, Peterson RE, Bushman W. Growth, morphogenesis, and differentiation during mouse prostate development in situ, in renal grafts, and in vitro. Prostate. 2005; 65:390–399. [PubMed: 16114054]

Frame FM, Pellacani D, Collins AT, Simms MS, Mann VM, Jones GD, Meuth M, Bristow RG, Maitland NJ. HDAC inhibitor confers radiosensitivity to prostate stem-like cells. Br J Cancer. 2013; 109:3023–3033. [PubMed: 24220693]

Glozak MA, Sengupta N, Zhang X, Seto E. Acetylation and deacetylation of non-histone proteins. Gene. 2005; 363:15–23. [PubMed: 16289629]

Grishina IB, Kim SY, Ferrara C, Makarenkova HP, Walden PD. BMP7 inhibits branching morphogenesis in the prostate gland and interferes with Notch signaling. Dev Biol. 2005; 288:334–347. [PubMed: 16324690]

Gryder BE, Akbashev MJ, Rood MK, Raftery ED, Meyers WM, Dillard P, Khan S, Oyelere AK. Selectively targeting prostate cancer with antiandrogen equipped histone deacetylase inhibitors. ACS Chem Biol. 2013; 8:2550–2560. [PubMed: 24004176]

Hogan BL. Bone morphogenetic proteins in development. Curr Opin Genet Dev. 1996; 6:432–438. [PubMed: 8791534]

Keil KP, Abler LL, Laporta J, Altmann HM, Yang B, Jarrard DF, Hernandez LL, Vezina CM. Androgen receptor DNA methylation regulates the timing and androgen sensitivity of mouse prostate ductal development. Dev Biol. 2014a

Keil KP, Abler LL, Mehta V, Altmann HM, Laporta J, Plisch EH, Suresh M, Hernandez LL, Vezina CM. DNA methylation of E-cadherin is a priming mechanism for prostate development. Dev Biol. 2014b; 387:142–153. [PubMed: 24503032]

Keil KP, Mehta V, Abler LL, Joshi PS, Schmitz CT, Vezina CM. Visualization and quantification of mouse prostate development by in situ hybridization. Differentiation. 2012a; 84:232–239. [PubMed: 22898663]

Keil KP, Mehta V, Branam AM, Abler LL, Buresh-Stiemke RA, Joshi PS, Schmitz CT, Marker PC, Vezina CM. Wnt inhibitory factor 1 (Wif1) is regulated by androgens and enhances androgen-dependent prostate development. Endocrinology. 2012b; 153:6091–6103. [PubMed: 23087175]

Lamm ML, Podlasek CA, Barnett DH, Lee J, Clemens JQ, Hebner CM, Bushman W. Mesenchymal factor bone morphogenetic protein 4 restricts ductal budding and branching morphogenesis in the developing prostate. Dev Biol. 2001; 232:301–314. [PubMed: 11401393]

Lin TM, Rasmussen NT, Moore RW, Albrecht RM, Peterson RE. Region-specific inhibition of prostatic epithelial bud formation in the urogenital sinus of C57BL/6 mice exposed in utero to 2,3,7,8-tetrachlorodibenzo-p-dioxin. Toxicol Sci. 2003; 76:171–181. [PubMed: 12944588]

Livak KJ, Schmittgen TD. Analysis of relative gene expression data using real-time quantitative PCR and the 2(-Delta Delta C(T)) Method. Methods. 2001; 25:402–408. [PubMed: 11846609]

Manson SR, Song JB, Hruska KA, Austin PF. HDAC dependent transcriptional repression of Bmp-7 potentiates TGF-beta mediated renal fibrosis in obstructive uropathy. J Urol. 2014; 191:242–252. [PubMed: 23820056]

Marks PA. The clinical development of histone deacetylase inhibitors as targeted anticancer drugs. Expert Opin Investig Drugs. 2010; 19:1049–1066.

Martinez G, Mishina Y, Bertram JF. BMPs and BMP receptors in mouse metanephric development: in vivo and in vitro studies. Int J Dev Biol. 2002; 46:525–533. [PubMed: 12141440]

Mehta V, Abler LL, Keil KP, Schmitz CT, Joshi PS, Vezina CM. Atlas of Wnt and R-spondin gene expression in the developing male mouse lower urogenital tract. Dev Dyn. 2011; 240:2548–2560. [PubMed: 21936019]

Mehta V, Schmitz CT, Keil KP, Joshi PS, Abler LL, Lin TM, Taketo MM, Sun X, Vezina CM. Beta-catenin (CTNNB1) induces Bmp expression in urogenital sinus epithelium and participates in prostatic bud initiation and patterning. Dev Biol. 2013; 376:125–135. [PubMed: 23396188]

Molife LR, Attard G, Fong PC, Karavasilis V, Reid AH, Patterson S, Riggs CE Jr, Higano C, Stadler WM, McCulloch W, Dearnaley D, Parker C, de Bono JS. Phase II, two-stage, single-arm trial of the histone deacetylase inhibitor (HDACi) romidepsin in metastatic castration-resistant prostate cancer (CRPC). Ann Oncol. 2010; 21:109–113. [PubMed: 19608618]

Omori A, Miyagawa S, Ogino Y, Harada M, Ishii K, Sugimura Y, Ogino H, Nakagata N, Yamada G. Essential roles of epithelial bone morphogenetic protein signaling during prostatic development. Endocrinology. 2014; 155:2534–2544. [PubMed: 24731097]

Patra SK, Patra A, Dahiya R. Histone deacetylase and DNA methyltransferase in human prostate cancer. Biochem Biophys Res Commun. 2001; 287:705–713. [PubMed: 11563853]

Pili R, Salumbides B, Zhao M, Altiok S, Qian D, Zwiebel J, Carducci MA, Rudek MA. Phase I study of the histone deacetylase inhibitor entinostat in combination with 13-cis retinoic acid in patients with solid tumours. Br J Cancer. 2012; 106:77–84. [PubMed: 22134508]

Prins GS, Huang L, Birch L, Pu Y. The role of estrogens in normal and abnormal development of the prostate gland. Ann N Y Acad Sci. 2006; 1089:1–13. [PubMed: 17261752]

Rathkopf D, Wong BY, Ross RW, Anand A, Tanaka E, Woo MM, Hu J, Dzik-Jurasz A, Yang W, Scher HI. A phase I study of oral panobinostat alone and in combination with docetaxel in patients with castration-resistant prostate cancer. Cancer Chemother Pharmacol. 2010; 66:181–189. [PubMed: 20217089]

Rathkopf DE, Picus J, Hussain A, Ellard S, Chi KN, Nydam T, Allen-Freda E, Mishra KK, Porro MG, Scher HI, Wilding G. A phase 2 study of intravenous panobinostat in patients with castration-resistant prostate cancer. Cancer Chemother Pharmacol. 2013; 72:537–544. [PubMed: 23820963]

Schneider BJ, Kalemkerian GP, Bradley D, Smith DC, Egorin MJ, Daignault S, Dunn R, Hussain M. Phase I study of vorinostat (suberoylanilide hydroxamic acid, NSC 701852) in combination with docetaxel in patients with advanced and relapsed solid malignancies. Invest New Drugs. 2012; 30:249–257. [PubMed: 20686817]

Sugimura Y, Cunha GR, Donjacour AA. Morphogenesis of ductal networks in the mouse prostate. Biol Reprod. 1986; 34:961–971. [PubMed: 3730488]

Vezina CM, Allgeier SH, Fritz WA, Moore RW, Strerath M, Bushman W, Peterson RE. Retinoic acid induces prostatic bud formation. Dev Dyn. 2008; 237:1321–1333. [PubMed: 18393306]

Wang X, Xu J, Wang H, Wu L, Yuan W, Du J, Cai S. Trichostatin A, a histone deacetylase inhibitor, reverses epithelial-mesenchymal transition in colorectal cancer SW480 and prostate cancer PC3 cells. Biochem Biophys Res Commun. 2015; 456:320–326. [PubMed: 25434997]

Weichert W, Roske A, Gekeler V, Beckers T, Stephan C, Jung K, Fritzsche FR, Niesporek S, Denkert C, Dietel M, Kristiansen G. Histone deacetylases 1, 2 and 3 are highly expressed in prostate cancer and HDAC2 expression is associated with shorter PSA relapse time after radical prostatectomy. Br J Cancer. 2008; 98:604–610. [PubMed: 18212746]

Xu RH, Peng Y, Fan J, Yan D, Yamagoe S, Princler G, Sredni D, Ozato K, Kung HF. Histone acetylation is a checkpoint in FGF-stimulated mesoderm induction. Dev Dyn. 2000; 218:628–635. [PubMed: 10906781]

Yang F, Chen Y, Shen T, Guo D, Dakhova O, Ittmann MM, Creighton CJ, Zhang Y, Dang TD, Rowley DR. Stromal TGF-beta signaling induces AR activation in prostate cancer. Oncotarget. 2014; 5:10854–10869. [PubMed: 25333263]

Zhang Y, Andl T, Yang SH, Teta M, Liu F, Seykora JT, Tobias JW, Piccolo S, Schmidt-Ullrich R, Nagy A, Taketo MM, Dlugosz AA, Millar SE. Activation of beta-catenin signaling programs embryonic epidermis to hair follicle fate. Development. 2008; 135:2161–2172. [PubMed: 18480165]

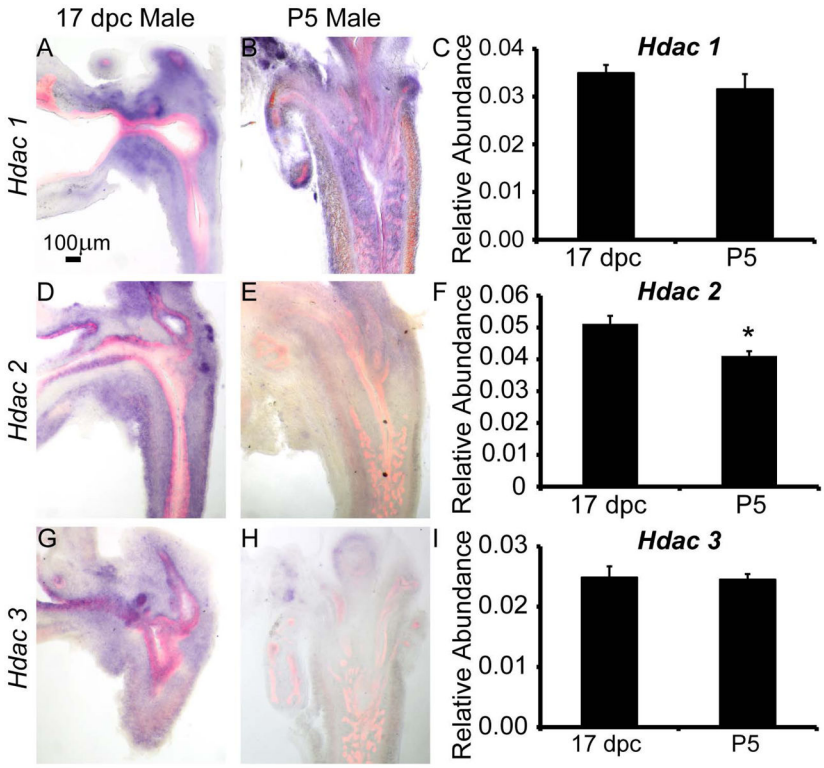

Figure 1. Type 1 histone deacetylase (*Hdac*) mRNAs are expressed and change in localization in fetal male mouse lower urinary tract during prostate budding and branching morphogenesis

In situ hybridization (ISH, purple) for *Hdac* mRNAs combined with immunohistochemistry (IHC) using antibodies targeting epithelium (E-cadherin, red) were used to pinpoint localization of (A–B) *Hdac1*, (D–E) *Hdac2* and (G–H) *Hdac3* in male mouse lower urinary tract sections from 17 days post coitus (dpc) and postnatal day (P)5. QPCR was used to determine relative abundance of *Hdac 1-3* mRNAs across whole male UGS at 17 dpc and P5 relative to a Ppi1 control (C,F,I). Results are mean ± SEM, n=5 mice per group. Asterisk indicates significant differences ($p \leq 0.01$) between groups.

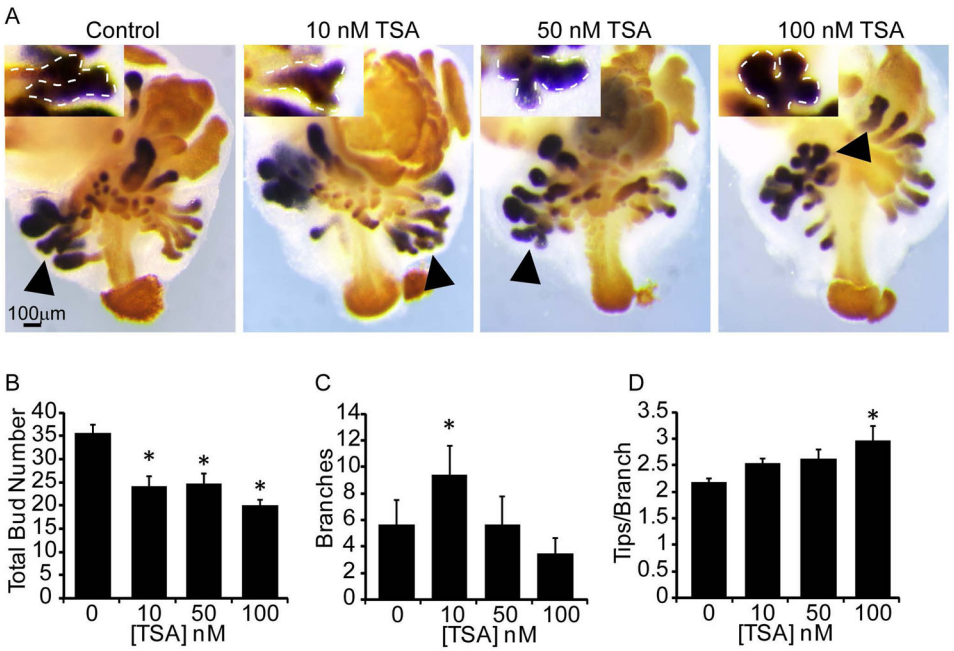

Figure 2. Chemical inhibition of histone deacetylases decreases prostatic bud number and alters branching morphogenesis in mouse UGS explant culture

14 dpc male mouse UGS explants were grown for 7 days in media containing androgen (10nM, dihydrotestosterone, DHT) and vehicle alone (0.1%DMSO) or vehicle containing trichostatin A (10–100nM TSA). (A) *In situ* hybridization was used to visualize NK3 transcription factor locus 1 (*Nkx3-1*, purple), which marks prostatic bud epithelium and immunohistochemistry (IHC) was used to visualize E-cadherin (orange), which marks UGS epithelium. (B) Prostatic bud number and (C) buds undergoing branching morphogenesis and (D) number of tips per bud undergoing branching morphogenesis were quantified from n=5 UGSs per group. Results are mean ± SEM. Asterisk indicates significant differences ($p \leq 0.05$) from control, arrowheads and insets indicate representative buds undergoing branching morphogenesis.

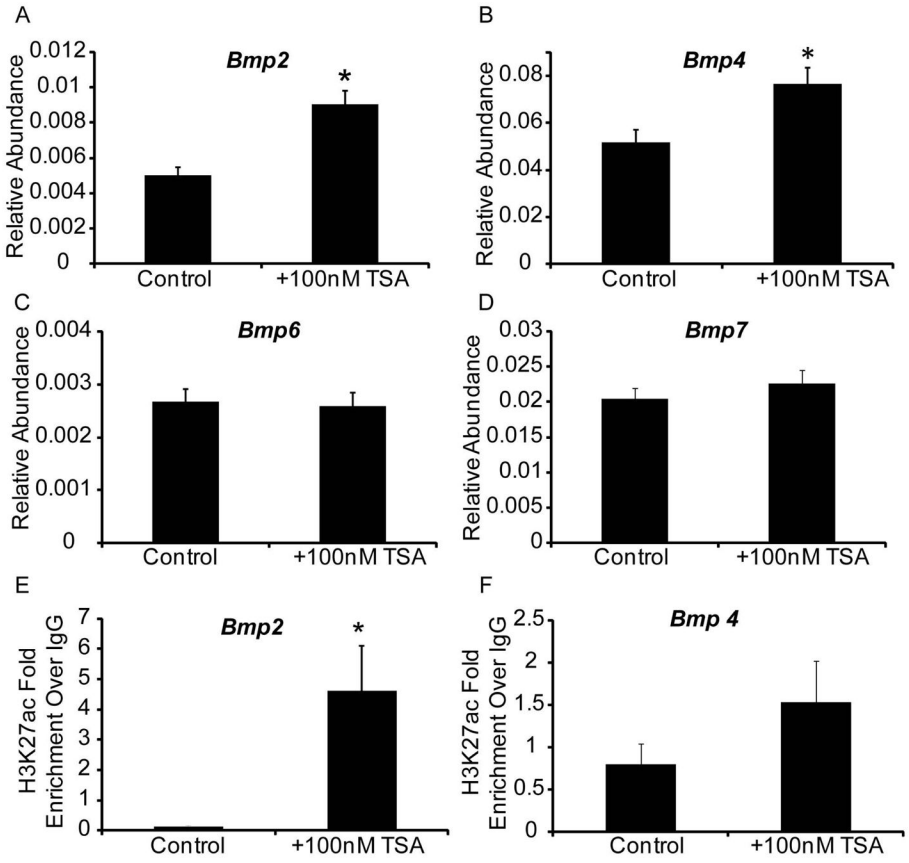

Figure 3. Chemical inhibition of histone deacetylases in mouse UGS explant culture increases *Bmp2* and *4* transcript abundance and enhances *Bmp2* histone acetylation

14 dpc male mouse UGS explants were grown for 7 days in media containing androgen (10nM, dihydrotestosterone, DHT) and vehicle alone (0.1%DMSO) or vehicle containing trichostatin A (100nM TSA). (A–D) Real time quantitative PCR (QPCR) was used to determine relative transcript abundance of *Bmp2*, *Bmp4*, *Bmp6* and *Bmp7*. (E–F) Chromatin immunoprecipitation (ChIP) was used to determine histone H3 lysine 27 acetylation (H3K27ac) at the *Bmp2* and *Bmp4* promoter region. Results are mean ± SEM. Asterisk indicates significant differences from control $p \leq 0.05$, n=5 per group.

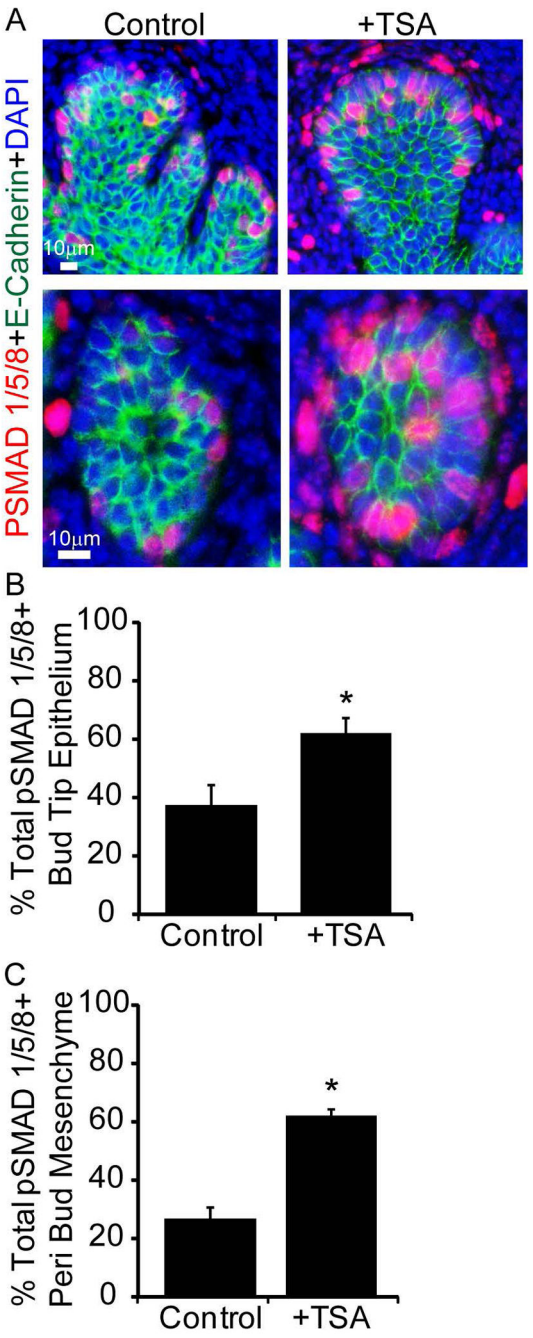

Figure 4. Chemical inhibition of histone deacetylation increases BMP target gene phosphoSMAD1/5/8 expression in epithelium and mesenchyme of mouse UGS explants

14 dpc male mouse UGS explants were grown for 7 days in media containing androgen (10nM, dihydrotestosterone, DHT) and vehicle alone (0.1%DMSO) or vehicle containing trichostatin A (100nM TSA). (A) Tissues were sectioned and stained with antibodies against BMP target gene phosphoSMAD1/5/8 (red), and E-cadherin (green). Nuclei were counterstained with DAPI. The percent of (B) pSMAD1/5/8 positive epithelial cells within prostatic bud tips and (C) pSMAD1/5/8 positive cells within mesenchyme surrounding

prostatic buds was quantified. Results are mean ± SEM. Asterisk indicates significant differences from control $p \leq 0.05$, n=5 per group.

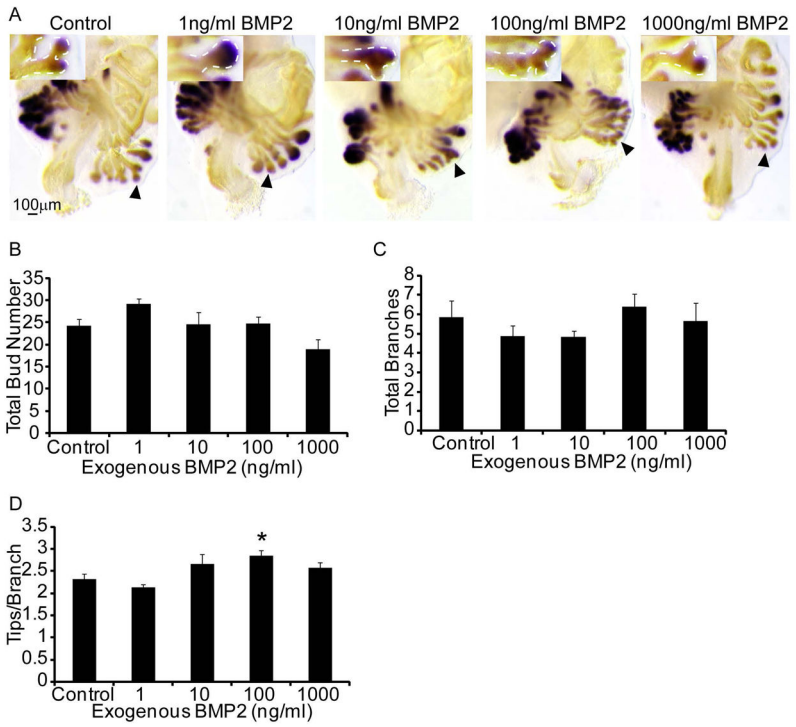

Figure 5. Exogenous BMP2 does not alter total prostatic bud number but causes excessive branching in prostatic buds undergoing branching morphogenesis

14 dpc male mouse UGS explants were grown for 7 days in media containing androgen (10nM, dihydrotestosterone, DHT) and increasing concentrations of exogenous recombinant human BMP2 (1–1000ng/ml). (A) Explants were stained as described in Fig. 2 to visualize prostatic buds. (B) Total prostatic bud number, (C) total prostatic buds undergoing branching morphogenesis and (D) number of terminal tips at the end of each branching prostatic bud were quantified. Results are mean ± SEM. Asterisk indicates significant differences from control $p \leq 0.05$, n=5 per group; arrowheads and insets indicate representative buds undergoing branching morphogenesis.

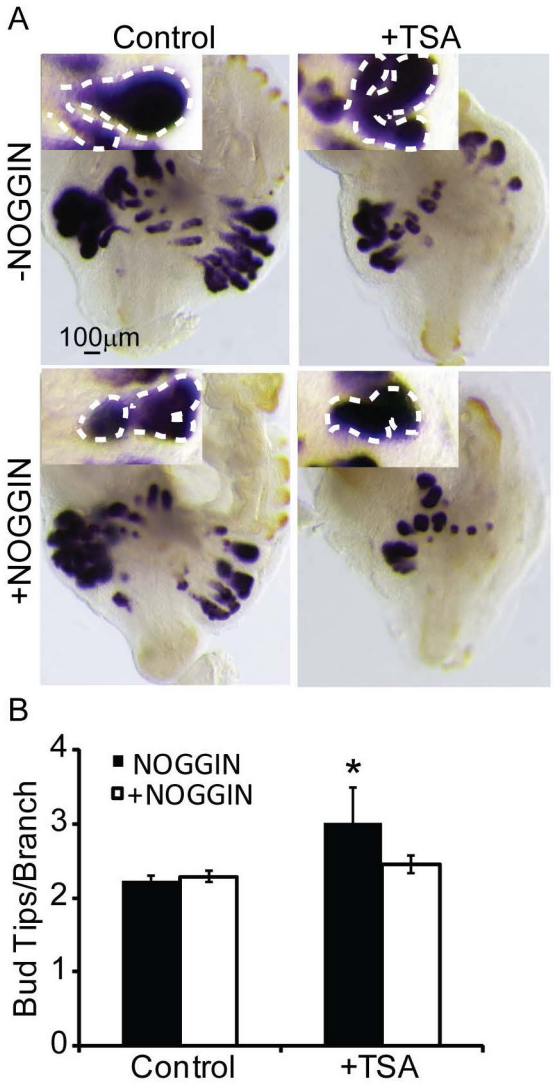

Figure 6. Inhibition of BMP signaling partially restores prostatic branching morphogenesis in UGS explants treated with a histone deacetylase inhibitor

14 dpc male mouse UGS explants were grown for 7 days in media containing androgen (10nM, dihydrotestosterone, DHT) and trichostatin A (100nM, TSA), recombinant NOGGIN (5μg/ml) or both. (A) Explants were stained as described in Fig. 2 to visualize prostatic buds. (B) The number of tips per branching bud was determined from the stained explants. Results are mean ± SEM. Asterisk indicates significant differences from control $p \leq 0.05$, n=5 per group; arrowheads and insets indicate representative buds undergoing branching morphogenesis.

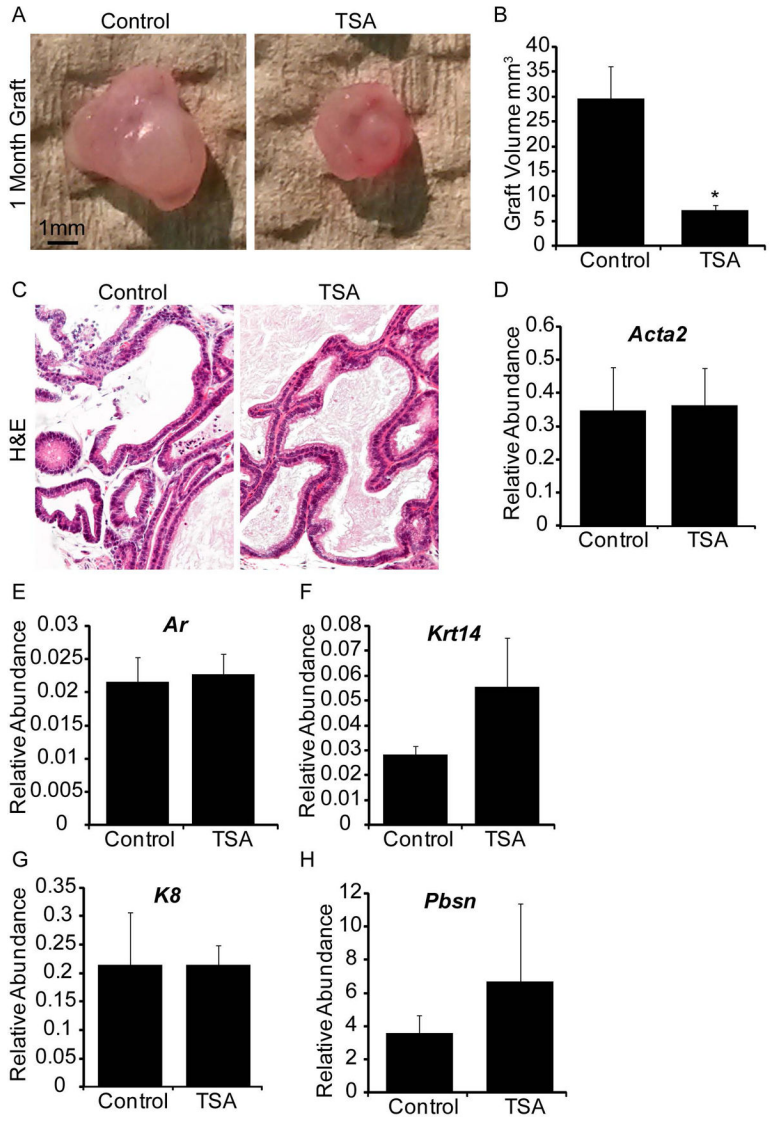

Figure 7. Inhibition of histone deacetylase-induced decreases in prostatic growth cannot be restored by renal grafting

14 dpc male prostate explants were grown for 7 days in media containing androgen (10nM, dihydrotestosterone, DHT) and trichostatin A (100nM, TSA). (A) Following culture tissues were transplanted under the renal capsule of a syngeneic adult intact male host mouse and allowed to grow for an additional month. After one month (B) graft volume and (C) hematoxolin and eosin staining were performed. Quantification by QPCR of (D) smooth muscle actin (*Acta2*), (E) androgen receptor (*Ar*), (F) cytokeratin 14 (*Krt14*), (G) cytokeratin 8 (*Krt8*) and (H) probasin (*Pbsn*) in explant grafts.

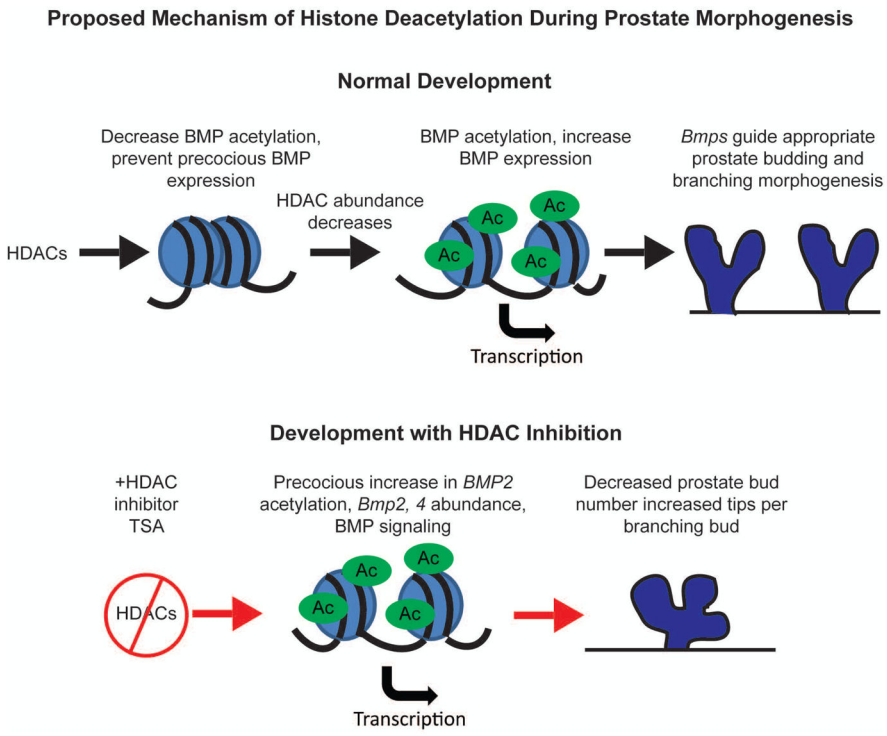

Figure 8. Proposed role of histone deacetylation in regulating BMP expression to shape prostate budding and branching morphogenesis

Over the course of prostate development HDAC expression decreases, relieving BMP repression leading to appropriate BMP expression to control prostate budding and branching morphogenesis. Inhibition of HDACs with TSA leads to inappropriate increase in *Bmp* acetylation and expression leading to decreased prostatic bud formation and a greater number of tips per branch in branching buds.

Table 1

Gene specific primers

Application	Entrez Gene ID	Gene	Genbank No.	Forward	Reverse
QPCR	11475	alpha actin 2, smooth muscle (acta2)	NM_007392.2	CTGCCGAGCGTGAGATTG	AATGAAAGATGGCTGGAAGAGAG
QPCR	11835	androgen Receptor (Ar)	NM_013476.3	GATGGTATTTGCCATGGGTTG	GGCTGTACATCCGAGACTTGTG
QPCR	12156	bone morphogenetic protein (Bmp2)	NM_007553.2	GGGCCCTCATAAAGAAGCAG	CTGCGTGTCAGGCAAATGTAG
QPCR	12159	bone morphogenetic protein 4 (Bmp4)	NM_007554.2	GCCATTGTGCAGACCCTAGTC	CAACATGGAAATGGCACTCAG
QPCR	12161	bone morphogenetic protein 6 (Bmp6)	NM_007556.2	AACCACGCCATTGTACAGACC	ACCGAGATGGCATTCAGTTTG
QPCR	12162	bone morphogenetic protein 7 (Bmp7)	NM_007557.2	GTAATCGCAAGCCTCGTTCAG	CAGTGGCTTCTGCTTGGTTTC
QPCR	268373	peptidylprolyl isomerase a (Ppia)	NM_ 008907	TCTCTCCGTAGATGGACCTG	ATCACGGCCGATGACGAGCC
QPCR	433759	histone deacetylase 1 (Hdac1)	NM_008228.2	TTATACCTTCCCACCCATCTTG	GAAGCTAGGCTATCAACCTCCAC
QPCR	15182	histone deacetylase 2 (Hdac2)	NM_008229.2	TCAGCAACCCTTGAATTTGAC	AATGTCCTCAAACAGGGAAGG
QPCR	15183	histone deacetylase 3 (Hdac3)	NM_010411.2	TCAGGGATGAGACATGGACAG	AAGGACAGAAGGAACAAATGAGG
QPCR	54192	probasin (Pbsn)	NM_017471	AATGTACAGCGTATCATGGAC	AAAGAGAAAGTACAGAGACAGG
QPCR	16691	keratin 8 (Krt8)	NM_031170.2	ATCCAACACTTTCAGCCGCAC	AAGACTCGGACACCAGCTTCC
QPCR	16664	keratin 14 (Krt14)	NM_016958	AATTCTCCTCTGGCTCTCAGTCATCC	AGCTTTAGTTCTTGGTGCGCAGGAC
QPCR	19701	renin 1 (Ren1)	NM_031192.3	CCTACGAGCTCCCTGAAGTTG	CCTCCCAGGTCAAAGGAAATG
QPCR	20234	spermine binding protein (Sbp1)	NM_011321.2	AGAGCCCAGAATGTCCTGGG	TTATCACGTGCTCTCCGTCC
ChIP QPCR	12156	bone morphogenetic protein 2 (Bmp2)	NM_007553.3	CCGACGACAGCAGCAGCCTT	AAGACTGGATCCGCCGGGCG
ChIP QPCR	12159	bone morphogenetic protein 4 (Bmp4)	NM_007554.2	GCCATTCCGTAGTGCCATTC	CATGATTCTTGGGAGCCAATC